BURNS 49 (2023) 1574–1584

Available online at www.sciencedirect.com

ScienceDirect

journal homepage: www.elsevier.com/locate/burns

Skeletal muscle wasting after burn is regulated by a decrease in anabolic signaling in the early flow phase

Dorien Dombrecht [a], *Ulrike Van Daele* [a,b,*], *Birgit Van Asbroeck* [a], *David R. Schieffelers* [a], *Pieter-Jan Guns* [c], *Eric van Breda* [a,**]

[a] *Department of Rehabilitation Sciences & Physiotherapy, Research Group MOVANT, University of Antwerp, Universiteitsplein 1, B-2610 Antwerp, Belgium*

[b] *Oscare, Organisation for Burns, Scar After-Care and Research, 2170 Antwerp, Belgium*

[c] *Laboratory of Physiopharmacology, University of Antwerp, Universiteitsplein 1, B-2610 Antwerp, Belgium*

ARTICLE INFO

Article history:
Accepted 10 August 2023

Keywords:
Burns
Muscle wasting
Skeletal muscle
Signaling pathways
Protein turnover

ABSTRACT

Following burns a sustained catabolic stress response is activated, resulting in skeletal muscle wasting. A better understanding of the underlying mechanisms of postburn skeletal muscle wasting is essential for the development of preventive and/or therapeutic strategies. Six weeks old female rats underwent a sham, 10% or 40% total body surface area scald burn. Ten days post-injury, severely burned animals gained significantly less weight compared to sham treated and minor burned animals, reflected in a significantly lower ratio of muscle to total body weight for Soleus (SOL) and Extensor Digitorum Longus (EDL) in the severely burned group. Postburn, total fiber number was significantly lower in EDL, while in SOL the amount of type1 fibers significantly increased and type2 fibers significantly decreased. No signs of mitochondrial dysfunction (COX/SDH) or apoptosis (caspase-3) were found. In SOL and EDL, eEF2 and pAKT expression was significantly lower after severe burn. MURF1,2,3 and Atrogin-1 was significantly higher in SOL, whilst in EDL MURF1,2,3 was significantly lower postburn. In both muscles, FOXO3A was significantly lower postburn. This study identified postburn changes in muscle anthropomorphology and proteins involved in pathways regulating protein synthesis and breakdown, with more pronounced catabolic effects in SOL.

1. Introduction

Skeletal muscle wasting is a prominent hallmark of the systemic stress response after a burn injury [1]. To improve functionality and quality of life of burn survivors, counteracting muscle wasting is highly important [2]. Although many facts of the metabolic consequences of burns are

* Corresponding author at: Department of Rehabilitation Sciences & Physiotherapy, Research Group MOVANT, University of Antwerp, Universiteitsplein 1, B-2610 Antwerp, Belgium.
** Corresponding author.
E-mail addresses:
ulrike.vandaele@uantwerpen.be (U. Van Daele),
eric.vanbreda@uantwerpen.be (E. van Breda).

https://doi.org/10.1016/j.burns.2023.08.011
0305-4179/

revealed, filling the gaps regarding underlying molecular mechanisms is crucial in the development of evidence based therapeutic strategies in burn rehabilitation [1,3].

Evidence supports that following a severe burn a sustained pathophysiological stress response is activated, characterized by persistent inflammatory and humoral stress responses, inducing a state of whole-body hypermetabolism, insulin resistance and muscle wasting up to nine months postburn [4–9]. However, to date, experimental studies are mainly focused on the acute effects of burns (one to five days postburn) [10,11]. Despite its systemic nature, skeletal muscle wasting is dependent on muscle fiber type [12]. Previous research shows that after burns predominantly type 2 muscles are more susceptible to muscle wasting compared with predominantly type 1 muscles [13,14].

Muscle wasting during the catabolic flow phase is, at the cellular level, a result of changes in intracellular signaling pathways adjusting to metabolic stimuli, resulting in a protein imbalance [15]. These pathways have been partly unraveled under various pathological conditions, such as in cancer and critical ill patients, but remain relatively unknown in burn patients [16,17]. Although it has been shown that during the catabolic phase postburn an increase in protein breakdown is one of the main causes of skeletal muscle wasting, literature concerning postburn protein synthesis is rather inconclusive [18,19]. Whereas some studies show a postburn increase in protein synthesis due to increased levels of free amino acids, other studies show a decrease due to different activation of intracellular pathways [20–22]. From other wasting conditions, it is known that one of the most important pathways determining the anabolic or catabolic state of a muscle is the PI3K-AKT pathway (*'phosphoinositide-3-kinase'-'Protein kinase B' (PKB)*), stimulated by anabolic hormones (Fig. 1) [23]. Downstream of PI3K, AKT phosphorylates a set of substrates, including mTORC1 *('mammalian target of rapamycin complex 1')* with downstream p70S6K *('Ribosomal protein S6 kinase')*, blocking apoptosis and inducing protein synthesis, gene transcription and cell proliferation [24]. Key downstream regulators of translation initiation signaling are eEF2 *('Eukaryotic elongation factor 2'),* stimulating RNA translation, and eIF2α ('Eukaryotic translation initiation factor 2α'), recognizing stress conditions [15,25,26].

Protein breakdown in skeletal muscle wasting is regulated by the Ubiquitin Proteasome System (UPS) and autophagy [17,27]. Key enzymes in proteasomal degradation are atrogenes MURF-1 *('muscle RING finger-1')* and Atrogin-1 (*'muscle atrophy F-box' (MAFbx)*), strongly upregulated in skeletal muscle wasting conditions [28,29]. Atrogene expression is regulated by various intracellular signaling pathways, including the PI3K-AKT pathway (Fig. 2) [24]. Also FOXOs *('Forkhead box protein O transcription factors')*, stimulated by decreases in insulin/IGF-1 and increases in inflammatory cytokines and glucocorticoids, play an important role in regulating the UPS and a number of essential autophagy related genes [15,30]. In many catabolic diseases apoptosis often precedes protein degradation in skeletal muscle [31].

Studies investigating the role of above-mentioned pathways in postburn muscle wasting are scarce [1,16]. We investigated Soleus muscle (SOL), with predominantly type 1 muscle fibers, and Extensor Digitorum Longus muscle (EDL), with predominantly type 2 muscle fibers, separately in a female rat burn model. To obtain a better understanding of affected signaling pathways, we analyzed pAKT, p70S6k, eIF2α and eEF2 for protein synthesis and FOXO3A, MURF-1 and Atrogin-1 for protein breakdown [15,27,30,32]. We hypothesize that after severe burns skeletal muscle wasting is caused by a protein imbalance resulting from altered expressions of protein synthesis regulating proteins and/or activation of atrogene transcription factors MURF-1 and Atrogin-1, induced by the inflammatory response in the postburn flow phase [33]. Besides, we hypothesize that postburn muscle wasting is regulated differently in type 1 and type 2 muscle fibers.

2. Material and methods

2.1. Animal model

All procedures were reviewed and approved by the Ethical Committee of laboratory animals of the University of Antwerp under number 2020–52. 30 female Sprague-Dawley rats (Charles River) of six weeks old were acclimated individually in specialized ventilation cabinets with a temperature of 22 °C ten days prior to burn injury. Rats were randomly assigned to one of three groups: (1) sham treatment (S; n = 10), (2) minor burn submitted to a 10% total body surface area (TBSA) burn (MB; n = 10) or (3) severe burn submitted to a 40% TBSA burn (SB; n = 10). Three animals were excluded from analysis for different reasons (death during anesthesia n = 1, hindlimb infections n = 1, burn size not according to protocol n = 1).

2.2. Burn model

Burns were inflicted according to the modified Walker-Mason model inflicting a deep dermal burn and inducing metabolic changes [34–36]. Animals were administered buprenorphine (0,05 mg/kg) (Temgesic, Schering-Plough, Belgium) and anaesthetized with 1–3% isoflurane (Zoetis, UK) in 100% oxygen. Next, rats were shaved with a clipper, placed in a mold exposing 10% (minor burn group) or 30% (severe burn group) TBSA of their back and submerged in 100 °C water for ten seconds [37]. An intraperitoneal injection of Ringers lactate was administered, rats were subsequently placed in a mold exposing 10% TBSA along their ventral side and submerged for three seconds in 100 °C water for the severe burn group and in room temperature water for the minor burn group. Sham treated rats underwent the same procedures but all in room temperature water. Rats were administered Ringers lactate 30 min, four hours and eight hours postburn (resulting in a total of 4 mL/kg/%TBSA) and buprenorphine 12 h postburn. Animals stayed in individual cages in specialized ventilation cabinets for the remainder of the experiment, received food and water ad libitum (Ssniff 'complete feed for rats & mice', consisting of 9% Fat, 24% Protein and 67% Carbohydrates) and were monitored daily using the Functional Observational Battery adjusted to the specific features of burns [38]. Animals showed normal ambulatory patterns without signals of pain.

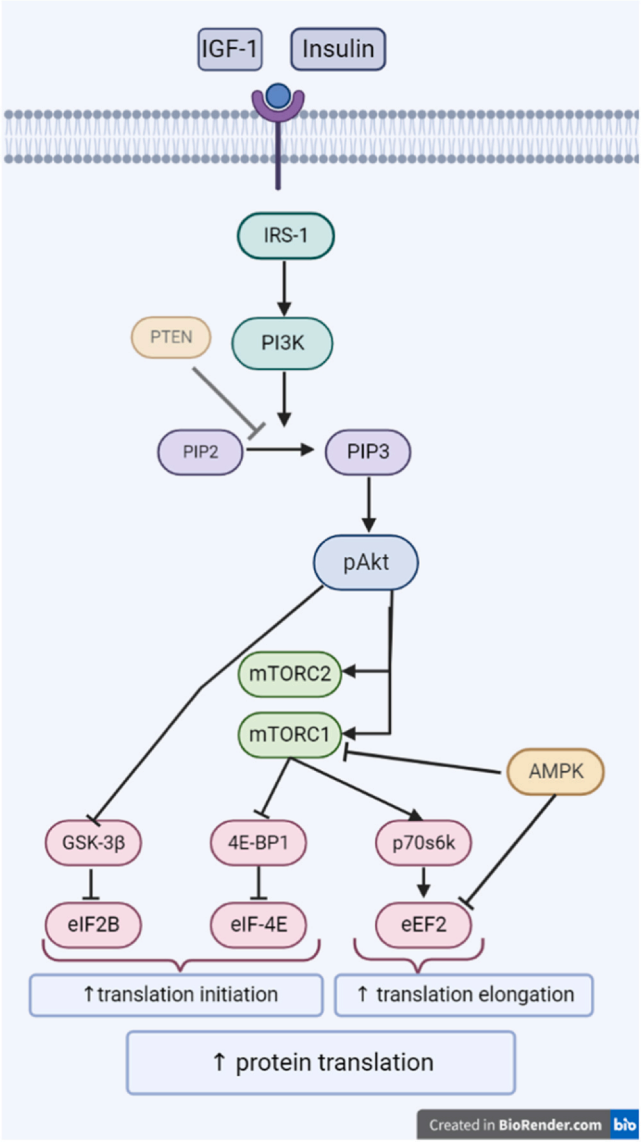

Fig. 1 – PI3K-AKT ('phosphoinositide-3-kinase'-'AKT') signaling pathway of protein synthesis in skeletal muscle. Upon Insulin or IGF-1 ('Insulin like growth factor-1) binding to its receptor, IRS-1 ('insulin receptor substrate 1′) activates PI3K, generates PIP3 ('phosphatidylinositol (3,4,5)-trisphosphate') at the plasma membrane, facilitating phosphorylation of AKT. Subsequently, downstream GSK-3β is inhibited (consequently inhibiting eIF2B) and parallel downstream mTORC1/2 ('mammalian target of rapamycin complex 1/2′) are activated, of which mTORC1 inhibits 4EBP1 ('eukaryotic initiation factor 4E binding protein') (consequently inhibiting eIF-4E ('Eukaryotic translation initiation factor 4E'), and stimulates p70s6k ('70 kDa ribosomal protein S6 kinase') (consequently inhibiting eEF2k which inhibits eEF2 ('translation initiation factor 2B')), resulting in the initiation of protein translation.

2.3. *Tissue collection*

Ten days after the burn procedure, animals were euthanized by an intraperitoneally injection of 250 mg/kg pentobarbital (Kela, Belgium). Animals were weighed, blood was immediately drawn by cardiac punction and hindlimb muscles (SOL and EDL) of both hindlimbs were harvested, weighed and one of each stored in a cryotube in liquid nitrogen. SOL and EDL from the other hindlimb of each animal were prepared for immunohistochemical analysis, placed on a cork, covered in Neg-50 Frozen Section Medium (Thermo Scientific, USA) and frozen in liquid nitrogen-cooled isopentane (2-methylbutane) (Honeywell, US). All samples were stored in a −80 °C freezer until further analysis.

2.4. *Immunohistochemistry*

Fiber type distribution (total fiber count, amount of type 1, type 2a and type 2b muscle fibers) was determined using a MyHC staining. Since this is a semi-qualitative technique it was performed on 6 (randomly chosen) muscles for each group. Unfixed transversal muscle sections (10 µm) were air-dried at room temperature and fixated with Paraformaldehyde (10 min). Slides

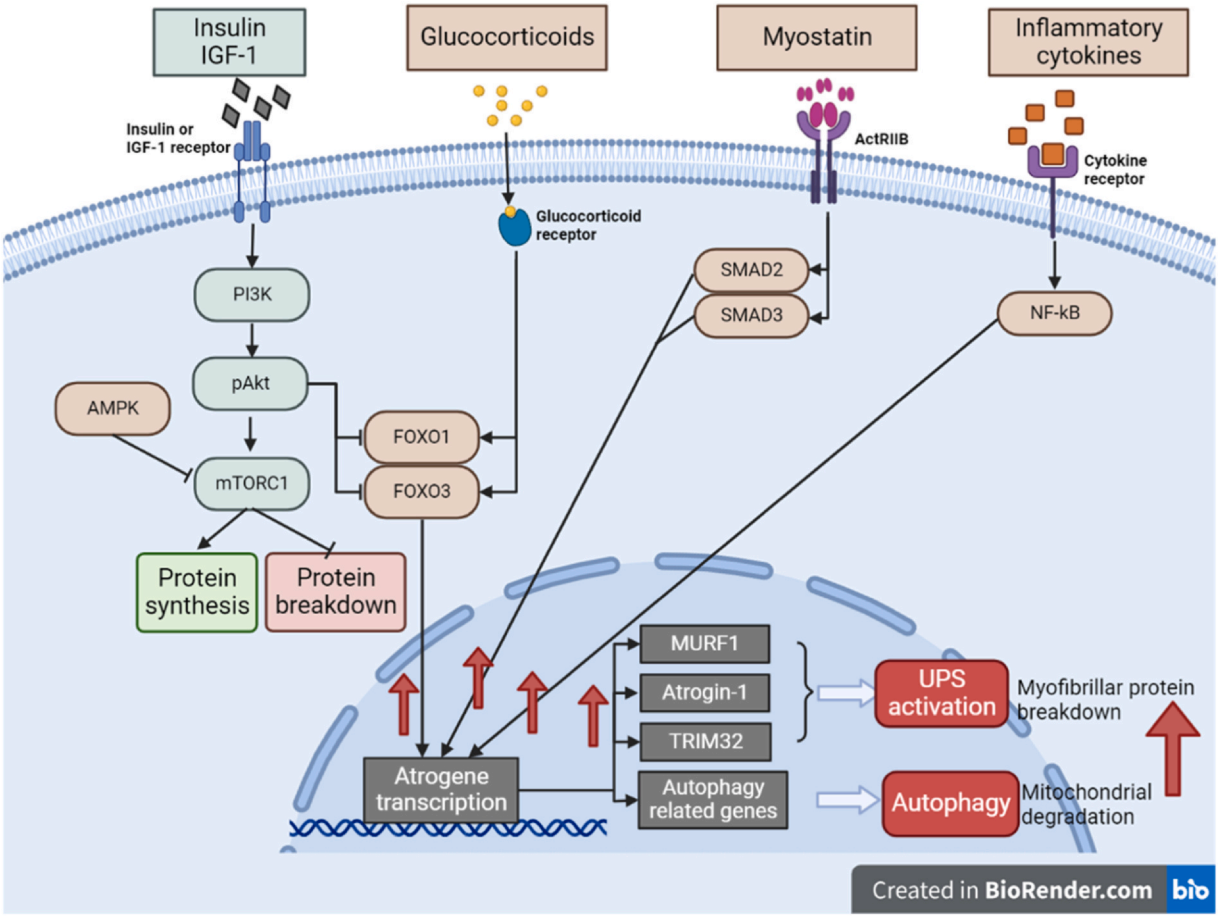

Fig. 2 – Main intracellular signaling pathways of skeletal muscle activating the UPS and Autophagy as found during other atrophy conditions. The atrogene transcription program is activated by 1) decreases in insulin or IGF-1 signaling, decreasing the activity of the PI3K-Akt-mTOR pathway, increasing expression of transcription factors FOXO1 and FOXO3; 2) increases in glucocorticoid release resulting in increases of FOXO1/3; 3) increased amounts of inflammatory cytokines leading to higher NF-κB expression; 4) transcription factors SMAD2 and SMAD3, stimulated by myostatin. The atrogene transcription program consequently leads to proteolysis via increased activity of MURF-1, atrogin-1, TRIM32 and autophagy related genes, stimulating the Ubiquitin Proteasome System (UPS) and Autophagy. IGF-1, insulin like growth factor 1; PI3K-Akt-mTOR, phosphoinositide 3-kinase-Akt-mammalian target of rapamycin; FOXO, forkhead box protein O; NF-κB, nuclear factor-κB; MURF-1, muscle-specific RING-finger 1; TRIM32, Tripartitie Motif Containing 32.

were pre-incubated with TBS-Tx, washed with TBS-T, blocked with horse serum (1:10) for 30 min and incubated overnight (at room temperature) with specific primary antibodies: anti-laminin (mouse; Bio-Techne NB300–144; 1:500) and isoform-specific myosin heavy chain (MyHC) antibodies: MyHC type 1 (BA-D5 mouse MIgG2b 1:5), MyHC type 2a (SC-71 mouse MIgG1 1:5) from Developmental Studies Hybridoma Bank (DSHB; Iowa City, IA, USA). Slides were washed in TBS-T and incubated for one hour with corresponding immunoglobulin-specific secondary antibodies were used: Alexa fluor 405 (anti-rabbit; Invitrogen A31553) IgG, Alexa fluor 555 (anti-mouse; Invitrogen A21147) IgG2b and Alexa fluor 633 (anti-mouse; Invitrogen A21126) IgG1. Afterwards, slides were washed in TBS-T, covered with 'Vectashield with DAPI' (Vector Laboratories) and air-dried. Images were taken at x10 magnification with a NIKON Eclipse Ti series high throughput fluorescent microscope and ImageJ software was used for further analysis.

To quantify apoptosis, slides were incubated with cleaved caspase-3 (cell signaling #9661, 1:300). To investigate mitochondrial dysfunction, the activity of the respiratory enzymes Cytochrome c oxidase (COX) and succinate dehydrogenase (SDH) was measured using the VitroView COX/SDH Double Histochemistry Stain kit (VB-3022) following manufacturer's instructions. Images were captured at x10 magnification with an Olympus BX43 microscope and analysed with ImageJ software.

Investigators were blinded to burn group for all histological analyses.

2.5. *Western blotting*

We determined, using Western Blotting, the expression of several key proteins 10 days after a severe burn injury, known to be involved in skeletal muscle wasting. Snap-

frozen SOL and EDL were collected in RIPA lysis buffer (Cell-Signaling, #9806) supplemented with phosphatase and protease inhibitor Tablets (Roche, 4906845001 and 11836170001: 1 Tablet of each/10 mL) in specially designed CK-28R tubes with 2.8 mm ceramic beads (Bertin Technologies P000916-LYSK0-A). A Precellys 24 (Bertin Technologies P000669-PR240-A) was used for tissue homogenization (6800 rpm for 3×30sec) and after centrifugation of the lysate (10 min at 14,000 rpm at 4 °C) protein suspension was extracted. Total protein concentration was quantitated using Pierce BCA Protein Assay kit (ThermoFisher #23225) following manufacturer's instructions. Diluted samples (1 µg/µl) were heat-denatured for five minutes at 100 °C.

Based on linear range analysis, 15 µg protein was loaded on Bolt 4–12% Bis-Tris gels (life technologies, NW04125BOX). Proteins were separated, transferred to a PVDF membrane. A total protein staining was performed using Revert 700 Total Protein Stain Kit (Li-COR biosciences, 926–11010). Membranes were scanned with an IR scanner (Odyssey Imaging System) and de-stained. Membranes were blocked in Intercept blocking buffer (Li-Cor Biosciences, 927–60001) and incubated overnight at 4 °C with the following rabbit IgG primary antibodies: anti-Akt1 (phospho S473; 1:1000; ab81283; Abcam)), anti-EEF2 (1:10000; ab75748; Abcam), anti-p70S6kinase (1:1000; 9202 Cell signaling), anti-eIF2α (1:1000; 9722 Cell signaling), Anti-MURF1 +MURF3 +MURF2 (1:1000; ab172479; Abcam), anti-Fbx32 (1:1000; ab168372; Abcam) and anti-FOXO3A (1:1000; ab23683; Abcam). After washing, a secondary anti-rabbit IgG IR-labeled secondary antibody (Li-COR LI 926–32211; 1:20000 dilution in Li-Cor blocking buffer supplemented with 0.01% SDS) was added for one hour and washed again. Membranes were imaged with an IR scanner (Odyssey imaging system). Analysis was completed with Empiria Studio software, and the signal from the protein bands was normalized to the Total Protein Stain signal.

2.6. Statistical analysis

Statistical analysis was performed using JMP-16. Experimental data for each burn group were expressed as means ± SEM. Differences between groups were analyzed using the Kruskal-Wallis test for general analysis and for immunohistological stainings. For western blots, linear mixed models was used, with the number of blots as a random effect to exclude technical variation between blots. Differences were considered to be statistically significant at $p < 0.05$.

3. Results

3.1. Total body mass and muscle weight

Severely burned animals gained significantly less body weight compared to sham treated (12 ± 3.2 g vs 27.8 ± 3.4 g; $p = 0.003$) and compared to minor burned animals (12 ± 3.2 g vs 22.7 ± 1.5 g; $p = 0.03$). Minor burned animals also gained less body weight compared to sham treated animals, although this difference was not significant ($p = 0.45$) (Fig. 3).

Muscle wet weights of both SOL and EDL were not significantly different between groups ($p = 0.09$ and $p = 0.47$ respectively) (Table 1). To account for differences in total body weight between the different groups at baseline, ratio of muscle wet weight-to-total body weight(baseline) was used. This ratio was significantly lower in severely burned animals compared with sham treated animals for both SOL (0.45 ± 0.01 vs 0.50 ± 0.01; $p = 0.03$) and EDL (0.47 ± 0.01 vs 0.54 ± 0.01; $p = 0.008$). In EDL, this ratio was also significantly lower in the severe burn group compared to the minor burn group (0.47 ± 0.01 vs 0.53 ± 0.01; $p = 0.02$) (Fig. 3).

3.2. Muscle morphology

Muscle fiber typing (Fig. 4) of SOL and EDL is shown in Fig. 5. In EDL total number of fibers is significantly lower in the severe burn compared to the sham treated group (177 ± 14 vs 237 ± 21; $p = 0.03$). In SOL a lower total fiber count was present in the severely burned animals compared to sham treated animals, but this was not significant ($p > 0.05$).

In SOL but not in EDL significant changes were found in type 1 and type 2 fiber distribution when comparing burn and sham treated groups. Number of type 1 muscle fibers was significantly higher in SOL of severely burned animals compared to both minor burned (87 ± 2 vs 77 ± 2; $p = 0.02$) and sham treated animals (87 ± 2 vs 76 ± 2; $p = 0.005$). Likewise, type 2 muscle fiber count was significantly lower in SOL of severely burned compared to minor burned animals (14 ± 2 vs 24 ± 2; $p = 0.005$), whereas the difference between severely burned and sham treated animals did not reach significance (14 ± 2 vs 22 ± 2; $p = 0.07$). Looking more specifically at type 2a and type 2b muscle fiber subdivision, number of type 2b fibers was significantly lower in severely burned compared to sham treated animals (0 ± 0 vs 1 ± 0; $p = 0.003$), whereas for the number of type 2a fibers no significant difference was found for severe vs sham treated animals (significance for SOL; $p = 0.0547$).

3.3. Mitochondrial oxidative activity and apoptosis

A COX/SDH staining was performed to evaluate mitochondrial oxidative capacity, but no COX negative fibers or red ragged fibers were found in SOL or EDL sections of sham treated, minor or severe burn animals. Further, a cleaved Caspase-3 staining showed no signs of apoptosis ten days post-injury.

3.4. Skeletal muscle protein synthesis: pAKT, p70S6K, eEF2 and eIF2α

eEF2 was significantly lower in SOL of severely burned animals compared to sham treated animals ($p < 0.0001$) (Fig. 6B). Also, the expression of pAKT and p70S6K in SOL was significantly lower in severely burned compared to sham treated animals ($p = 0.003$ and $p = 0.044$, respectively) (Fig. 6C and E). In EDL eEF2, pAKT, p70S6K and eIF2α were significantly lower in severely burned animals compared to sham treated animals ($p < 0.0001$, $p = 0.005$, $p = 0.015$ and $p = 0.044$ respectively) (Fig. 6F-I).

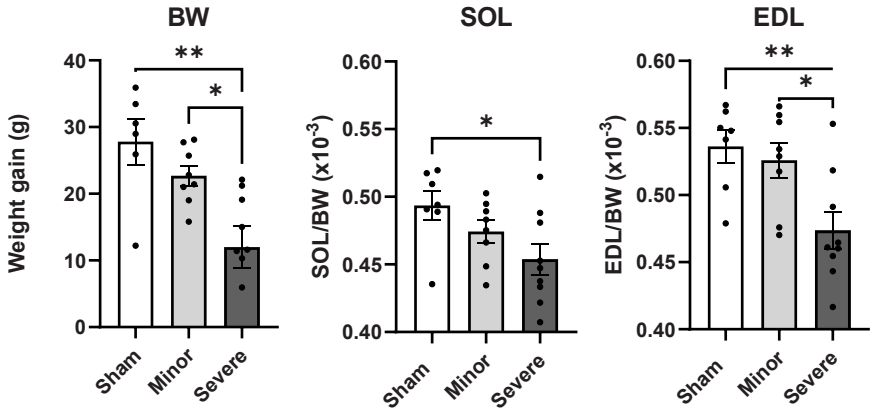

Fig. 3 – Difference in total body weight (BW) gain (weight day 10 minus weight day 0 postburn), ratio of m. Soleus (SOL) and m. Extensor Digitorum Longus (EDL) wet weight (mg) at 10 days postburn to total body weight at baseline (BW) (g) for sham, minor and severe burned animals. N = 9 per group, error bars represent SEM, significant difference $^{*}p < 0.05$, $^{**}p < 0.01$.

Table 1 – Total body weight(g) at baseline and 10 days postburn (end) and wet weights (mg) of m. Soleus (SOL) and m. Extensor Digitorum Longus (EDL) 10 days postburn. Values are expressed as mean ± SEM. N = 9 per group. *significant difference vs sham; #significant difference vs minor burn group; Significance if p < 0.05.

	Body weight baseline (g)	Body weight end (g)	Body weight gain (g)	SOL (mg)	EDL (mg)
Sham	200.7 ± 8.7	228.5 ± 6.4	27.8 ± 3.4	96.1 ± 4.3	104 ± 4.7
Minor burn	194.5 ± 2.6	217.2 ± 2.2	22.7 ± 1.5	89.5 ± 3.3	99.4 ± 4
Severe burn	227 ± 7.2#*	239 ± 7.5#	12 ± 3.2#*	103.4 ± 5.3	107.8 ± 5.5

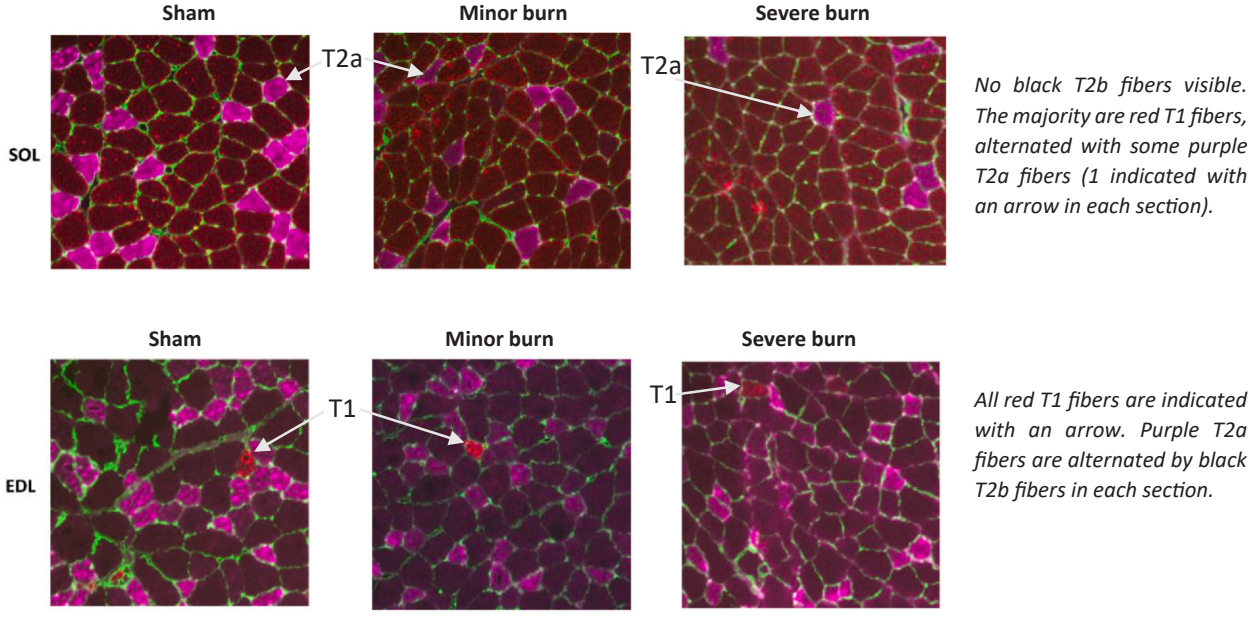

No black T2b fibers visible. The majority are red T1 fibers, alternated with some purple T2a fibers (1 indicated with an arrow in each section).

All red T1 fibers are indicated with an arrow. Purple T2a fibers are alternated by black T2b fibers in each section.

Fig. 4 – Example of the used immunohistology MyHC staining on transversal muscle sections (10 µm) of sham treated, minor and severely burned Soleus (SOL) muscle samples and ~~on~~ of sham treated, minor and severely burned Extensor Digitorum (EDL) muscle samples captured at 10x magnification. Green indicates the basal membrane, red type 1 fibers, purple type 2a fibers and black type 2b fibers.

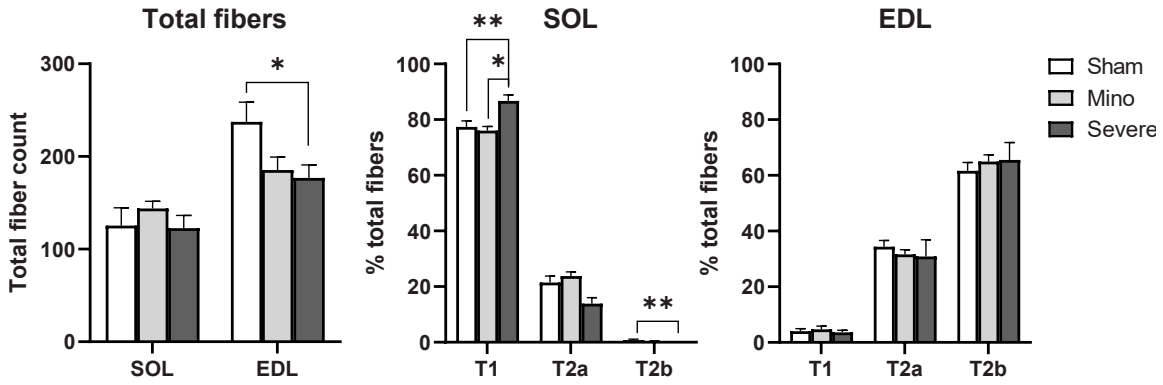

Fig. 5 – Muscle fiber type distribution: total fiber count, % of type 1 (T1), type 2a (T2a) and type 2b (T2b) fibers (specific fiber type count/total fiber count) for Soleus (SOL) and Extensor Digitorum Longus (EDL) transversal muscle sections (10 µm) from sham treated, minor and severe burned animals after 10 days. N = 6 per group, error bars represent SEM, Significant difference $^{*}p < 0.05$, $^{**}p < 0.01$.

3.5. *Skeletal muscle protein breakdown: MURF-1, Atrogin-1 and FOXO3A*

In SOL, both MURF-1 and Atrogin-1 were higher 10 days after the severe burn, however only the difference in Atrogin-1 was significant ($p = 0.002$) (Fig. 7A-B). FOXO3A showed a significant lower expression in the severely burned group compared to the sham treated group ($p = 0.01$) (Fig. 7C). In EDL of severely burned animals, we found a significant lower expression of both MURF-1 ($p = 0.02$) and FOXO3A ($p = 0.0004$) compared to sham treated animals (Fig. 7D and F). No significant difference was found for Atrogin-1 in EDL of severely burned animals compared to sham treated animals ($p = 0.41$) (Fig. 7E).

4. Discussion

The purpose of this study was to investigate the effects of burns on skeletal muscle, including pathways affecting protein synthesis and breakdown. We found changes in body weight, muscle weight and muscle morphology 10 days postburn, consistent with previous observations both in rats [11,12,39–41] and humans [5,42,43]. Besides, we demonstrated that the expression of different proteins involved in signaling pathways that regulate skeletal muscle protein balance was altered postburn, but interestingly not all key signaling proteins appear affected. To date, experimental studies are mainly focused on the acute effects of burns on clinical parameters like (lean) body mass, muscle force and overall protein content [11–13,40,44]. The Walker-Mason burn model for rats was used, which induces a hypermetabolic response similar as in humans [45–47]. Davenport et al. confirmed that using this model, full thickness burns were created with a predefined surface area, making this the most suitable model for in-depth burn research [48].

4.1. *Body weight and skeletal muscle morphology*

Ten days postburn we found a significant lower body weight gain compared to sham treated animals, which is consistent with observations in other studies [12,45,46]. This difference correlates to the severity of the burn injury, where a higher %TBSA led to a lower body weight gain. We also observed, in line with other investigations, a lower ratio of muscle wet weight to body weight, suggesting that lower body weight gain is most likely due to less lean body mass, and thus skeletal muscle mass [10,39,40].

We found a decrease in total number of fibers in EDL after severe burn, supporting the hypothesis that after a burn injury type 2 (fast-twitch) muscles are more prone to muscle wasting after burns than type 1 (slow-twitch) muscles. In SOL, muscle fibers shifted towards more type 1 (slow-twitch) fibers. These findings are in line with other catabolic conditions such as sepsis, starvation, cachexia and aging [13,49], but are in contrast with conditions such as microgravity and hindlimb unloading, where previous research has shown a switch from type 1 to type 2 fibers [50,51]. Although we have no clear explanation for these differences, other studies have suggested that the difference in metabolic response between type 1 and type 2 muscle fibers is caused by a more pronounced upregulation of the ubiquitin proteolytic pathway in fast-twitch muscles, causing muscle catabolism [13,14]. Because of these discrepancies, we investigated the effect of burns on skeletal muscle protein regulation in predominantly type 1, EDL, and type 2, SOL, muscles separately.

4.2. *Regulation of skeletal muscle protein metabolism after burns*

Since no clear anthropomorphic changes were found 10 days after minor burns, we decided not to perform Western Blots for the muscles of minor burned animals. We found a lower expression of both pAKT, p70S6K and eEF2 in both SOL and EDL in comparison to sham treated animals. These findings are similar to distorted pathways in other cachectic diseases such as cancer [16,17]. The lower pAKT after burns is indicative for a decreased activation of the PI3/AKT pathway, presumably due to endocrine disturbances [52]. Lower p70S6K indicates lower mTOR signaling postburn [43]. These findings are of major importance since the PI3K/AKT

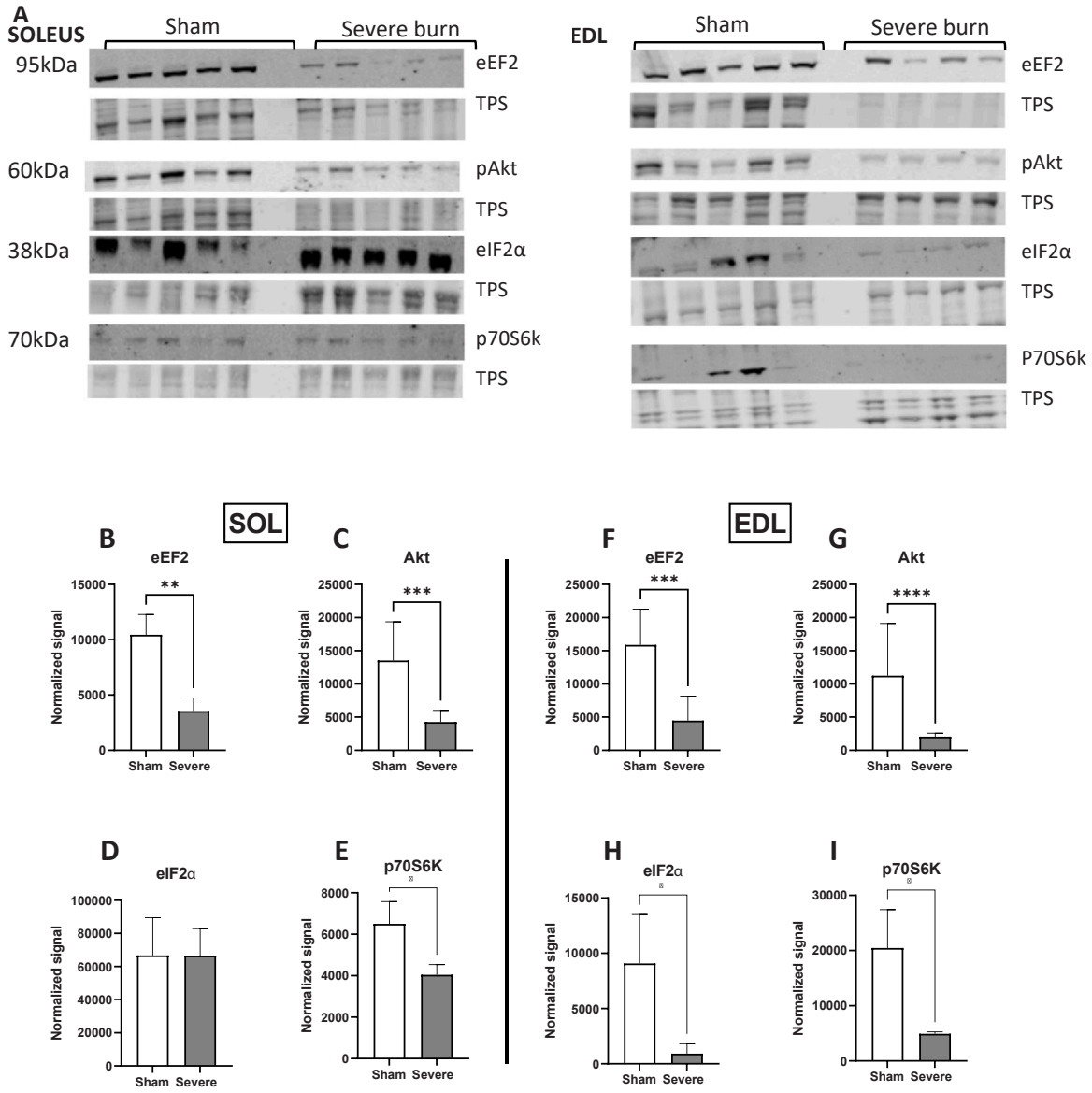

Fig. 6 – A: Western blots for eEF2, Akt, eIF2α and p70S6K of Soleus (SOL) and Extensor Digitorum Longus (EDL) muscle. The immunoblots depicted are representative of samples of sham treated and severely burned animals 10 days post injury. For every protein, the Total Protein Stain (TPS) at the corresponding molecular height is depicted. B-I: Protein signals of Western blots normalized to Total protein stains in sham treated versus severe burn groups 10 days postburn. Bars represent SEM. A-E: Normalized protein signals in SOL F-I: Normalized protein signals in EDL. N = 9 per group, error bars represent SEM, significant difference $^{**}p < 0.01$, $^{****}p < 0.0001$.

pathway is one of the most important pathways determining the anabolic or catabolic state of skeletal muscle [24]. In addition, protein synthesis can be affected independent of the PI3K/AKT pathway by downstream proteins, such as eEF2. In contrast to our results, Song et al. found that total eEF2 was not altered in pediatric burn patients (at 10 and 49 days postburn) suggesting a non-canonical role for eEF2 [42]. eIF2α was found only to be lower in EDL postburn, but not in SOL. Although it is not easy to comprehend the reason for different expression of eIF2α in EDL and SOL postburn, our findings confirm the speculations of Rios-Fuller et al. that the pathological regulation of eIF2α is muscle type specific[53].

Surprisingly, we did not find a higher expression of MURF-1, Atrogin-1 and FOXO3A in muscle samples of severely burned animals. Only Atrogin-1 in SOL showed a significant higher expression 10 days after the burn injury. Previous studies have shown that energy-ubiquitin-dependent proteolysis, regulated by MURF-1 and Atrogin-1, is stimulated after burn injuries [10]. For instance, Quintana et al. have shown a higher MURF-1 and Atrogin-1 expression in Gastrocnemius muscle [41], whereas Lang et al. have showed that also at mRNA level both E3 ligases are upregulated after burns [11]. One factor that might explain the discrepancies between our findings and these studies are the different

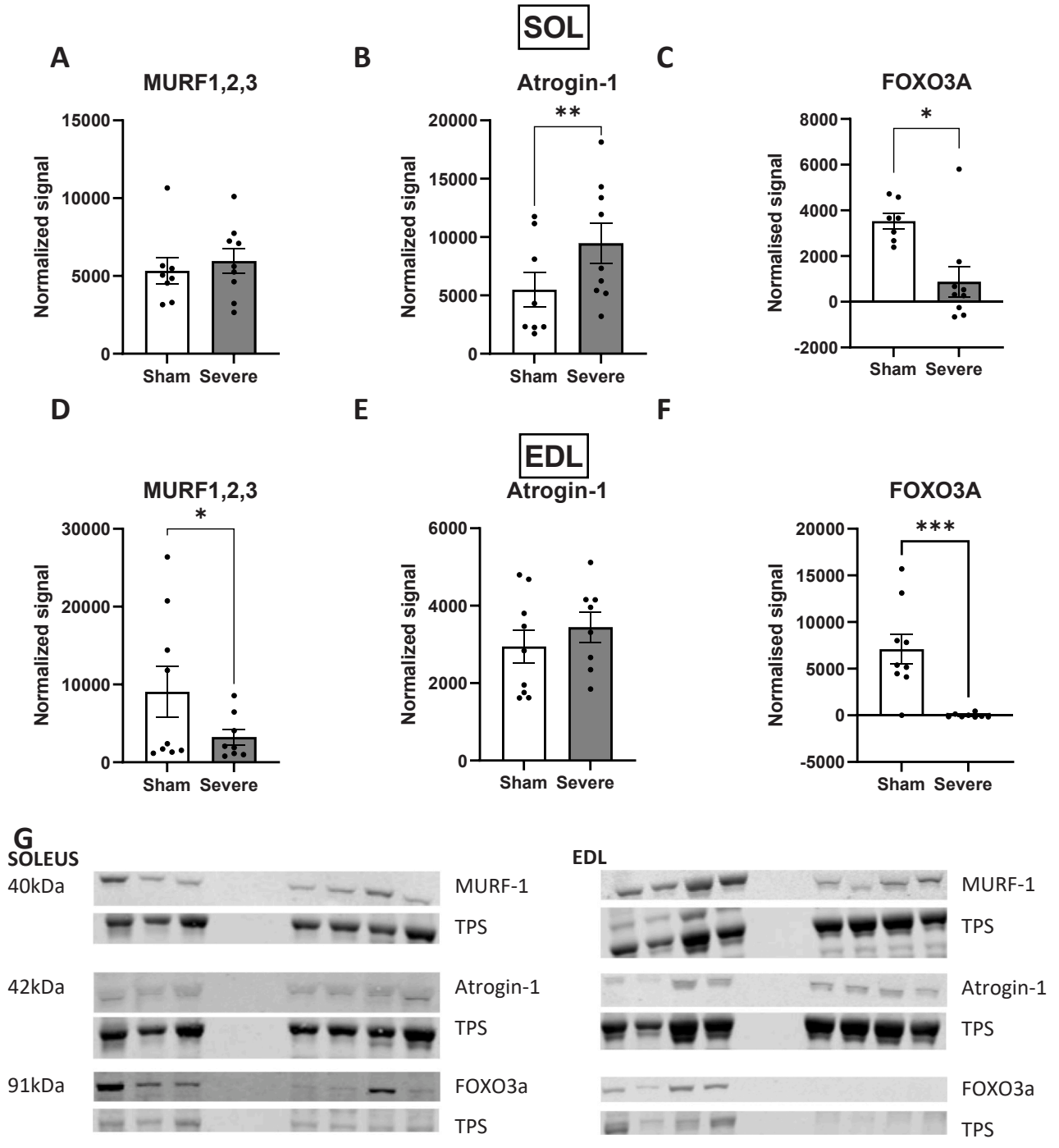

Fig. 7 – Protein signals of Western blots normalized to Total protein stains in sham versus severe burn groups 10 days postburn. Bars represent SEM. A. Normalized MURF1,2,3 protein signal in Soleus muscle. B. Normalized Atrogin-1 protein signal in Soleus muscle. C. Normalized FOXO3A protein signal in Soleus muscle D. Normalized MURF1,2,3 protein signal in EDL muscle. E. Normalized Atrogin-1 protein signal in EDL muscle. F. Normalized FOXO3A protein signal in EDL muscle. G. Western blots for MURF1,2,3, Atrogin-1 and FOXO3A of Soleus and Extensor Digitorum Longus muscle. The immunoblots depicted are representative of samples of sham and severely burned animals 10 days post injury. For every protein, the Total Protein Stain (TPS) at the corresponding molecular height is depicted. N = 9 per group, error bars represent SEM, significant difference $^{*}p < 0.05$, $^{**}p < 0.01$, $^{***}p < 0.001$.

measurement timepoints, i.e. 10 days postburn, well into the flow-phase, compared to 48 h until four days postburn in the above mentioned studies. Therefore, based on these findings, we hypothesize that both E3 ligases are upregulated postburn but in type 1 or mixed muscles the increases are sustained over a longer period of time.

4.3. *Mitochondrial oxidative activity and apoptosis*

There is no agreement as to the role of apoptosis in postburn skeletal muscle wasting. Previous studies reported an increase in apoptosis in skeletal muscle postburn, while our results showed no increase in caspase-3 activity either in SOL or EDL [40,54]. However, our results are in agreement with the studies by Duan et al., reporting that caspase-3 levels decreased to basal levels at day 10 postburn, and by Merritt et al., reporting no significant increases in activated caspases during the postburn flow phase [40,43]. We assume that the contribution of apoptosis to muscle wasting after burns is important in the first few days after the burn injury, as Duan et al. found marked increases in caspase-3 levels on one and four days postburn [40]. It should be noted that apoptosis has been shown to be upregulated in immobilization an sedentary behavior, which also contributes to muscle wasting after burns, but was not taken into account in the present study [55,56].

On muscle sections of the burned animals, COX/SDH staining revealed no positive fibers. Positive complexes II (SDH) and IV (COX) would indicate mitochondrial impairments encoded by both nuclear and mitochondrial DNA (mtDNA)[57]. Our results indicate that at 10 days postburn the nuclear DNA, encoding SDH, is not impaired and that there are no mutations of the mitochondrial DNA, encoding subunits of COX. This is in contrast to previous studies in cancer cachexia, where loss of oxidative phenotype and mitochondrial content was found concomitant with muscle wasting [58]. Even after sepsis impaired mitochondrial complex enzymes have been observed long after the sepsis has resolved, shown by lower complex II and complex IV activity [59].

5. Conclusion

In conclusion, we have shown that at 10 days postburn changes in muscle anthropometry are present and that proteins related to signaling pathways regulating protein synthesis and protein breakdown are altered, with more pronounced catabolic effects in SOL. In both SOL and EDL anabolic signaling was clearly reduced postburn. Overall, our findings support the idea that severe burns lead to a protein imbalance, induced by metabolic changes altering intracellular signaling pathways. This understanding may help to guide future research to elucidate the relative contribution of pathways and molecules leading to postburn muscle wasting in the postburn flow phase.

Funding

DD is funded through a doctoral fellowship by the 'Bijzonder Onderzoeks Fonds' (BOF) from the University of Antwerp [BOF39963].

Declaration of Competing Interest

The authors declare that they have no conflict of interest.

REFERENCES

[1] Dombrecht D, Van Daele U, Van Asbroeck B, Schieffelers D, Guns PJ, Gebruers N, et al. Molecular mechanisms of post-burn muscle wasting and the therapeutic potential of physical exercise. J Cachexia Sarcopenia Muscle 2023.
[2] Porter C, Hardee JP, Herndon DN, Suman OE. The role of exercise in the rehabilitation of patients with severe burns. Exerc Sport Sci Rev 2015;43(1):34–40.
[3] Porter C, Tompkins RG, Finnerty CC, Sidossis LS, Suman OE, Herndon DN. The metabolic stress response to burn trauma: current understanding and therapies. Lancet 2016;388(10052):1417–26.
[4] Jeschke MG, Gauglitz GG, Kulp GA, Finnerty CC, Williams FN, Kraft R, et al. Long-term persistance of the pathophysiologic response to severe burn injury. PLoS One 2011;6(7):e21245.
[5] Hart DW, Wolf SE, Mlcak R, Chinkes DL, Ramzy PI, Obeng MK, et al. Persistence of muscle catabolism after severe burn. Surgery 2000;128(2):312–9.
[6] Gauglitz GG, Herndon DN, Kulp GA, Meyer III WJ, Jeschke MG. Abnormal insulin sensitivity persists up to three years in pediatric patients post-burn. J Clin Endocrinol Metab 2009;94(5):1656–64.
[7] Izamis M-L, Uygun K, Uygun B, Yarmush ML, Berthiaume F. Effects of burn injury on markers of hypermetabolism in rats. J Burn Care Res 2009;30(6):993–1001.
[8] Chao T, Herndon DN, Porter C, Chondronikola M, Chaidemenou A, Abdelrahman DR, et al. Skeletal muscle protein breakdown remains elevated in pediatric burn survivors up to one-year post-injury. Shock 2015;44(5):397–401.
[9] Stanojcic M, Abdullahi A, Rehou S, Parousis A, Jeschke MG. Pathophysiological response to burn injury in adults. Ann Surg 2018;267(3).
[10] Fang CH, Tiao G, James H, Ogle C, Fischer JE, Hasselgren PO. Burn injury stimulates multiple proteolytic pathways in skeletal muscle, including the ubiquitin-energy-dependent pathway. J Am Coll Surg 1995;180(2):161–70.
[11] Lang CH, Huber D, Frost RA. Burn-induced increase in atrogin-1 and MuRF-1 in skeletal muscle is glucocorticoid independent but downregulated by IGF-I. Am J Physiol Regul Integr Comp Physiol 2007;292(1):R328–36.
[12] Wu X, Baer LA, Wolf SE, Wade CE, Walters TJ. The impact of muscle disuse on muscle atrophy in severely burned rats. J Surg Res 2010;164(2):e243–51.
[13] Fang CH, Li BG, Tiao G, Wang JJ, Fischer JE, Hasselgren PO. The molecular regulation of protein breakdown following burn injury is different in fast- and slow-twitch skeletal muscle. Int J Mol Med 1998;1(1):163–9.
[14] Wu X, Wolf SE, Walters TJ. Muscle contractile properties in severely burned rats. Burns 2010;36(6):905–11.
[15] Glass DJ. Signalling pathways that mediate skeletal muscle hypertrophy and atrophy. Nat Cell Biol 2003;5(2):87–90.
[16] Bowen TS, Schuler G, Adams V. Skeletal muscle wasting in cachexia and sarcopenia: molecular pathophysiology and impact of exercise training. J Cachexia Sarcopenia Muscle 2015;6(3):197–207.
[17] Cohen S, Nathan JA, Goldberg AL. Muscle wasting in disease: molecular mechanisms and promising therapies. Nat Rev Drug Discov 2015;14(1):58–74.
[18] Gordon BS, Kelleher AR, Kimball SR. Regulation of muscle protein synthesis and the effects of catabolic states. Int J Biochem Cell Biol 2013;45(10):2147–57.
[19] Pereira C, Murphy K, Jeschke M, Herndon DN. Post burn muscle wasting and the effects of treatments. Int J Biochem Cell Biol 2005;37(10):1948–61.
[20] Sommerhalder C, Blears E, Murton AJ, Porter C, Finnerty C, Herndon DN. Current problems in burn hypermetabolism. Curr Probl Surg 2020;57(1):100709.
[21] Biolo G, Fleming RY, Maggi SP, Nguyen TT, Herndon DN, Wolfe RR. Inverse regulation of protein turnover and amino acid

transport in skeletal muscle of hypercatabolic patients. J Clin Endocrinol Metab 2002;87(7):3378–84.
[22] Fong YM, Minei JP, Marano MA, Moldawer LL, Wei H, Shires 3rd GT, et al. Skeletal muscle amino acid and myofibrillar protein mRNA response to thermal injury and infection. Am J Physiol 1991;261(3 Pt 2):R536–42.
[23] Sartorelli V, Fulco M. Molecular and cellular determinants of skeletal muscle atrophy and hypertrophy. Sci STKE 2004;2004(244):re11.
[24] Glass DJ. PI3 kinase regulation of skeletal muscle hypertrophy and atrophy. Curr Top Microbiol Immunol 2010;346:267–78.
[25] Anthony TG. Mechanisms of protein balance in skeletal muscle. Domest Anim Endocrinol 2016;56(Suppl):S23–32. (Suppl).
[26] Miyake M, Nomura A, Ogura A, Takehana K, Kitahara Y, Takahara K, et al. Skeletal muscle-specific eukaryotic translation initiation factor 2α phosphorylation controls amino acid metabolism and fibroblast growth factor 21-mediated non-cell-autonomous energy metabolism. FASEB J 2016;30(2):798–812.
[27] Bonaldo P, Sandri M. Cellular and molecular mechanisms of muscle atrophy. Dis Model Mech 2013;6(1):25–39.
[28] Goll DE, Neti G, Mares SW, Thompson VF. Myofibrillar protein turnover: the proteasome and the calpains. J Anim Sci 2008;86(14 Suppl):E19–35.
[29] Cao PR, Kim HJ, Lecker SH. Ubiquitin-protein ligases in muscle wasting. Int J Biochem Cell Biol 2005;37(10):2088–97.
[30] Stitt TN, Drujan D, Clarke BA, Panaro F, Timofeyva Y, Kline WO, et al. The IGF-1/PI3K/Akt pathway prevents expression of muscle atrophy-induced ubiquitin ligases by inhibiting FOXO transcription factors. Mol Cell 2004;14(3):395–403.
[31] Argilés JM, López-Soriano FJ, Busquets S. Apoptosis signalling is essential and precedes protein degradation in wasting skeletal muscle during catabolic conditions. Int J Biochem Cell Biol 2008;40(9):1674–8.
[32] Fanzani A, Conraads VM, Penna F, Martinet W. Molecular and cellular mechanisms of skeletal muscle atrophy: an update. J Cachexia Sarcopenia Muscle 2012;3(3):163–79.
[33] Jeschke MG, Chinkes DL, Finnerty CC, Kulp G, Suman OE, Norbury WB, et al. Pathophysiologic response to severe burn injury. Ann Surg 2008;248(3):387–401.
[34] Walker HL, Mason Jr. AD. A standard animal burn. J Trauma 1968;8(6):1049–51.
[35] Venter NG, Monte-Alto-Costa A, Marques RG. A new model for the standardization of experimental burn wounds. Burns 2015;41(3):542–7.
[36] Joshi AP, Saad MK, Mohan M, editors. A review on burn and burn models in animals. 2017.
[37] Gouma E, Simos Y, Verginadis I, Lykoudis E, Evangelou A, Karkabounas S. A simple procedure for estimation of total body surface area and determination of a new value of Meeh's constant in rats. Lab Anim 2012;46(1):40–5.
[38] Mathiasen JR, Moser VC. The Irwin test and Functional Observational Battery (FOB) for assessing the effects of compounds on behavior, physiology, and safety pharmacology in rodents. Curr Protoc Pharm 2018;83(1):e43.
[39] Chai J, Wu Y, Sheng Z. The relationship between skeletal muscle proteolysis and ubiquitin-proteasome proteolytic pathway in burned rats. Burns 2002;28(6):527–33.
[40] Duan H, Chai J, Sheng Z, Yao Y, Yin H, Liang L, et al. Effect of burn injury on apoptosis and expression of apoptosis-related genes/proteins in skeletal muscles of rats. Apoptosis 2009;14(1):52–65.
[41] Quintana HT, Baptista VIA, Lazzarin MC, Antunes HKM, Le Sueur-Maluf L, de Oliveira CAM, et al. Insulin modulates myogenesis and muscle atrophy resulting from skin scald burn in young male rats. J Surg Res 2021;257:56–68.
[42] Song J, Finnerty CC, Herndon DN, Kraft R, Boehning D, Brooks NC, et al. Thermal injury activates the eEF2K-dependent eEF2 pathway in pediatric patients. JPEN J Parent Enter Nutr 2012;36(5):596–602.
[43] Merritt EK, Cross JM, Bamman MM. Inflammatory and protein metabolism signaling responses in human skeletal muscle after burn injury. J Burn Care Res 2012;33(2):291–7.
[44] Gore DC, Chinkes DL, Wolf SE, Sanford AP, Herndon DN, Wolfe RR. Quantification of protein metabolism in vivo for skin, wound, and muscle in severe burn patients. JPEN J Parent Enter Nutr 2006;30(4):331–8.
[45] Herndon DN, Wilmore DW, Mason Jr. AD. Development and analysis of a small animal model simulating the human postburn hypermetabolic response. J Surg Res 1978;25(5):394–403.
[46] Barrow RE, Meyer NA, Jeschke MG. Effect of varying burn sizes and ambient temperature on the hypermetabolic rate in thermally injured rats. J Surg Res 2001;99(2):253–7.
[47] Wolfe RR. Review: acute versus chronic response to burn injury. Circ Shock 1981;8(1):105–15.
[48] Davenport L, Dobson G, Letson H. A new model for standardising and treating thermal injury in the rat. MethodsX 2019;6:2021–7.
[49] Wang Y, Pessin JE. Mechanisms for fiber-type specificity of skeletal muscle atrophy. Curr Opin Clin Nutr Metab Care 2013;16(3):243–50.
[50] Caiozzo VJ, Haddad F, Baker MJ, Herrick RE, Prietto N, Baldwin KM. Microgravity-induced transformations of myosin isoforms and contractile properties of skeletal muscle (1985). J Appl Physiol 1996;81(1):123–32.
[51] Desplanches D, Mayet MH, Sempore B, Flandrois R. Structural and functional responses to prolonged hindlimb suspension in rat muscle (1985). J Appl Physiol 1987;63(2):558–63.
[52] Sugita H, Kaneki M, Sugita M, Yasukawa T, Yasuhara S, Martyn JA. Burn injury impairs insulin-stimulated Akt/PKB activation in skeletal muscle. Am J Physiol Endocrinol Metab 2005;288(3):E585–91.
[53] Rios-Fuller TJ, Mahe M, Walters B, Abbadi D, Pérez-Baos S, Gadi A, et al. Translation regulation by eIF2α phosphorylation and mTORC1 signaling pathways in non-communicable diseases (NCDs). Int J Mol Sci 2020;21(15).
[54] Yasuhara S, Perez ME, Kanakubo E, Yasuhara Y, Shin YS, Kaneki M, et al. Skeletal muscle apoptosis after burns is associated with activation of proapoptotic signals. Am J Physiol Endocrinol Metab 2000;279(5):E1114–21.
[55] Allen DL, Linderman JK, Roy RR, Bigbee AJ, Grindeland RE, Mukku V, et al. Apoptosis: a mechanism contributing to remodeling of skeletal muscle in response to hindlimb unweighting. Am J Physiol 1997;273(2 Pt 1):C579–87.
[56] Zhu S, Nagashima M, Khan MA, Yasuhara S, Kaneki M, Martyn JA. Lack of caspase-3 attenuates immobilization-induced muscle atrophy and loss of tension generation along with mitigation of apoptosis and inflammation. Muscle Nerve 2013;47(5):711–21.
[57] Ross JM. Visualization of mitochondrial respiratory function using cytochrome c oxidase/succinate dehydrogenase (COX/SDH) double-labeling histochemistry. J Vis Exp 2011(57):e3266.
[58] Brown JL, Rosa-Caldwell ME, Lee DE, Blackwell TA, Brown LA, Perry RA, et al. Mitochondrial degeneration precedes the development of muscle atrophy in progression of cancer cachexia in tumour-bearing mice. J Cachexia Sarcopenia Muscle 2017;8(6):926–38.
[59] Owen AM, Patel SP, Smith JD, Balasuriya BK, Mori SF, Hawk GS, et al. Chronic muscle weakness and mitochondrial dysfunction in the absence of sustained atrophy in a preclinical sepsis model. eLife 2019:8.